

See discussions, stats, and author profiles for this publication at: <https://www.researchgate.net/publication/7459100>

Photonic Crystal Aqueous Metal Cation Sensing Materials

ARTICLE *in* ANALYTICAL CHEMISTRY · APRIL 2003

Impact Factor: 5.64 · DOI: 10.1021/ac026328n · Source: PubMed

CITATIONS

95

READS

45

4 AUTHORS:



Sanford A Asher

University of Pittsburgh

312 PUBLICATIONS **13,108** CITATIONS

SEE PROFILE



Anjal C. Sharma

Lynntech Inc.

7 PUBLICATIONS **812** CITATIONS

SEE PROFILE



Alexander V. Goponenko

University of Nebraska at Lincoln

21 PUBLICATIONS **912** CITATIONS

SEE PROFILE



Michelle M Ward Muscatello

University of Pittsburgh

10 PUBLICATIONS **269** CITATIONS

SEE PROFILE

Photonic Crystal Aqueous Metal Cation Sensing Materials

Sanford A. Asher,* Anjal C. Sharma, Alexander V. Goponenko, and Michelle M. Ward

Department of Chemistry, Chevron Science Center, University of Pittsburgh, Pittsburgh, Pennsylvania 15260

We developed a polymerized crystalline colloidal array photonic material that senses metal cations in water at low concentrations (PCCACS). Metal cations such as Cu^{2+} , Co^{2+} , Ni^{2+} , and Zn^{2+} bind to 8-hydroxyquinoline groups covalently attached to the PCCACS. At low metal concentrations ($< \mu\text{M}$), the cations form bisliganded complexes with two 8-hydroxyquinolines that cross-link the hydrogel and cause it to shrink, which blue shifts the photonic crystal diffraction. These bisliganded cross-links break at higher cation concentrations due to the formation of monoliganded cation complexes. This red shifts the diffraction. We have extended hydrogel volume phase transition theory in order to quantitatively model the diffraction dependence upon metal concentration. These materials can be used as a dosimeter to sense extremely low metal cation concentrations or as a sensor material for concentrations greater than $1 \mu\text{M}$. Metal cation concentrations can be determined visually from the color of the diffracted light or can be determined by reflectance measurements using a spectrophotometer. This sensing material could be used in the field to visually determine metal cation concentrations in drinking water. A color chart would be used to relate the diffracted color to the metal cation concentration.

There is a need for simple, inexpensive sensors for species such as metal cations in water.¹ For example, one important application would be to evaluate drinking water purity.^{1,2} It would be most useful if these sensors could be utilized to determine water quality in the field without requiring instrumentation.^{1,2} At present, most of the U.S. Environmental Protection Agency (EPA) methods³ to determine metal ion levels in water sources require significant instrumentation, are expensive, and are nonportable. Most methods utilize inductively coupled plasma, atomic absorption, or emission spectroscopy.

Newer methods of determining metal cations utilize complexing agents whose fluorescence monitors metal cation concentrations.^{4–7} The advantages of this approach are that high-temperature atomization sources are not required and that the fluorescence instrumentation can be miniaturized for use in the field. A disadvantage is that many of these complexation agents bind cations effectively only in partially organic environments.^{4–6} This may require sample preparation in the field.

Alternatively, cations such as Ag^+ and Hg^{2+} have been determined by using PVC immobilized dithiocarbamate sensor materials where cation binding results in absorption spectral changes.¹ Similar absorption sensors were fabricated by immobilizing absorbing ionophores on Nafion membranes to determine Cu^{2+} in tap water.² It is possible to miniaturize absorption spectral instruments for use in the field.

Recently, the utility of ion-selective electrodes (ISEs) has increased significantly. ISEs can now selectively detect metal ions such as Pb^{2+} , Ca^{2+} , Cd^{2+} , and K^+ in water⁶ and appear capable of providing the selectivities and sensitivities for trace metal ion determinations required by the EPA.⁸ These ISEs can be fabricated into small, portable, rugged sensors, and their electrochemical circuitry can be fabricated into small, portable, battery-operated devices. Thus, we conclude that there are a number of inexpensive and moderately expensive approaches for determining metal cation concentrations of water in the field.

We demonstrate in this paper the development of an inexpensive, new, sensing material, which can be used to visually determine ultralow concentrations of cations such as Cu^{2+} , Zn^{2+} , and Co^{2+} in aqueous media. The reflected color of this sensor material depends sensitively upon the aqueous cation concentration. This sensor material is based on our previously developed polymerized crystalline colloidal array (PCCA) photonic crystal sensing materials. These PCCA sensing materials (Figure 1) utilize a mesoscopically periodic array of colloidal particles,^{9–14} polym-

* To whom correspondence is to be addressed. Phone: 412-624-8570. Fax: 412-624-0588. E-mail: asher@pitt.edu.

- (1) Lerchi, M.; Reitter, E.; Simon, W.; Pretsch, E.; Chowdhury, D. A.; Kamata, S. *Anal. Chem.* **1994**, *66*, 1713–1717.
- (2) Sands, T. J.; Cardwell, T. J.; Cattrall, R. W.; Farrell, J. R.; Iles, P. J.; Kolev, S. D. *Sens. Actuators, B* **2002**, *85*, 33–41.
- (3) Guidelines establishing test procedures for the analysis of pollutants under the Clean Water act; national primary drinking water regulations; and national secondary drinking water regulations; methods update. *Fed. Regist.* **2001**, *66*, 3466–3497.

- (4) Czarnik, A. W. *Acc. Chem. Res.* **1994**, *27*, 302–308 and references therein.
- (5) Hayashita, T.; Terame, N.; Kuboyama, T.; Nakamura, S.; Yamamoto, H.; Nakamura, H. *J. Inclusion Phenom. Mol. Recognit. Chem.* **1998**, *32*, 251–265 and references therein.
- (6) Bronson, R. T.; Bradshaw, J. S.; Savage, P. B.; Fuangwasdi, S.; Lee, S. C.; Krakowiak, K. E.; Izzatt, R. M. *J. Org. Chem.* **2001**, *66*, 4752–4758.
- (7) Telting-Diaz, M.; Bakker, E. *Anal. Chem.* **2002**, *74*, 5251–5256.
- (8) Bakker, E.; Pretsch, E. *Anal. Chem.* **2002**, *74*, 420A–426A and references therein.
- (9) Asher, S. A.; Flaugh, P. L.; Washingier, G. *Spectroscopy* **1986**, *1*, 26–31.
- (10) Carlson, R. J.; Asher, S. A. *Appl. Spectrosc.* **1984**, *38*, 297–304.
- (11) Weissman, J. M.; Sunkara, H. B.; Tse, A. S.; Asher, S. A. *Science* **1996**, *274*, 959–960.

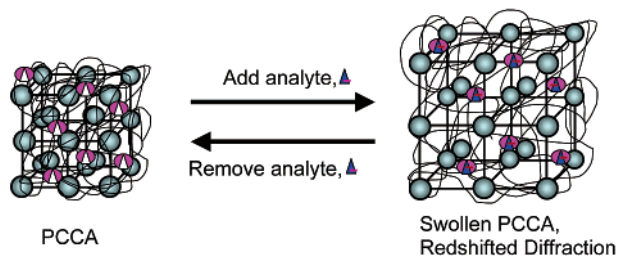


Figure 1. Crystalline colloidal arrays (CCA) formed because of electrostatic repulsion between particles. The spacings are ~ 200 nm, such that they diffract visible light. Polymerized CCA (PCCA) are formed by polymerizing a cross-linked hydrogel network around the CCA. The hydrogel is functionalized with a molecular recognition agent, which interacts with the analyte to actuate either shrinking or swelling. This alters the CCA spacing, which shifts the diffracted wavelength and changes the apparent color.

erized into an acrylamide hydrogel^{15–18} to diffract light in the visible spectral region.^{9–18} This PCCA also contains molecular recognition agents; when an analyte binds to the recognition group, it actuates a PCCA volume change in proportion to the analyte concentration.^{15–18} The resulting diffraction wavelength shifts cause visually evident color changes. Thus, the diffracted wavelength reports on the identity and concentration of the target analyte.

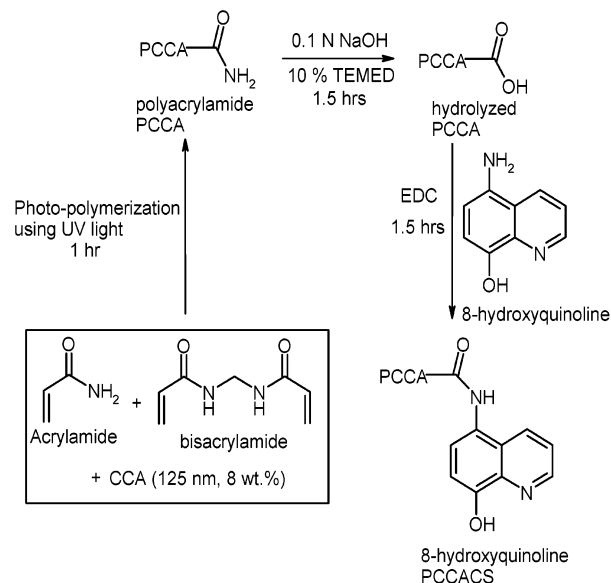
Our new sensing material utilizes 8-hydroxyquinoline as the recognition group for metal cations. These PCCA 8-hydroxyquinoline sites bind to cations such as Cu^{2+} , Co^{2+} , and Zn^{2+} . Thus, this sensor detects the presence of a wide array of cations in water.

EXPERIMENTAL SECTION

Synthesis of 5-Acetamido-8-hydroxyquinoline Hydrochloride. 5-Amino-8-hydroxyquinoline dihydrochloride (0.2961 g, 1.26 mmol, Aldrich) was dissolved in 100 mL of Nanopure water. The pH of the solution was adjusted to 7.0 by dropwise addition of 20% v/v aqueous NaOH (Fisher) solution. This solution was extracted with three 100-mL aliquots of CH_2Cl_2 (Fisher), and the combined extracts were dried over anhydrous Na_2SO_4 (5 g, 35.20 mmol, Fisher) for 2 h. After filtration, the CH_2Cl_2 stirred extract was cooled to 0°C in an ice bath and acetyl chloride (1.26 mmol, 0.100 mL, Acros) was slowly added dropwise over 1 min. The orange solution immediately turned dark purple, and a brownish orange flocculant rapidly formed. The reaction was stirred in the ice bath for 15 min and at room temperature for 1 h. The precipitate was filtered, washed once with 25 mL of CH_2Cl_2 , and three times with 25-mL portions of ethyl ether (Fisher).

The isolated precipitate was air-dried overnight and characterized using NMR (0.245 g, 82% yield). ^1H NMR (D_2O , Cambridge

Scheme 1. Preparation of 8-Hydroxyquinoline-Appended PCCA Cation Sensor Material



Isotopes): δ 2.135 (s, 3H, acetyl $-\text{CH}_3$), 7.15 (d, 1H, o-arom phenolic ring $-\text{H}$), 7.41 (d, 1H, m-arom phenolic ring $-\text{H}$), 7.85 (dd, 1H, m-arom pyridyl ring $-\text{H}$), 8.79 (d, 1H, p-arom pyridyl ring $-\text{H}$), 8.85 (s, 1H, o-arom pyridyl ring $-\text{H}$). The phenolic $-\text{OH}$ and the amide $>\text{NH}$ were not observed, most likely due to D_2O exchange. ^{13}C NMR (D_2O , Cambridge Isotopes): δ 22.38 (1C, acetyl $-\text{CH}_3$), 116.15, 122.35, 124.4, 126.57, 128.98, 142.95, 143.28, 146.57 (9 C, arom C), 175.00 (1C, acetamido carbonyl $=\text{C}=\text{O}$). An alternative synthesis of this compound was previously described.¹⁹

Synthesis of Cation Sensor Material. Scheme 1 depicts the PCCACS synthesis: Acrylamide (0.10 g, 1.4 mmol, Bio-Rad), *N,N*-methylenebisacrylamide (0.05 g, 0.32 mmol, Fluka), colloid suspension (2.00 g, 8% w/w dispersion, polystyrene latex spheres, 130-nm diameter)^{9–18} in Nanopure water, AG 501-X8 (D) ion-exchange resin (~ 0.1 g, 20–50 mesh, mixed bed, Bio-Rad), and 10% DEAP (7.7 μL , 3.84 μmol ; DEAP, diethoxyacetophenone; Aldrich) in DMSO (Fisher) were mixed in a 2-dram sample vial. The mixture was injected between two quartz disks separated by a Parafilm spacer (125 μm thick). The crystalline colloidal array (CCA) self-assembled to give a diffracting liquid film. This film was photopolymerized into a polymerized CCA (PCCA) by exposure for 1 h to UV light from two mercury lamps (Blak Ray) with their maximum intensity at 365 nm. The cell was opened, and the PCCA was washed thoroughly with pure water. The PCCA was cut into four pieces and stored in pure water (diffraction maximum ~ 720 nm).

The PCCA was hydrolyzed at room temperature for 90 min by placing it in NaOH (25 mL, 0.1 N, Fisher) solution in 10% v/v aqueous *N,N,N,N*-tetramethylethylenediamine (TEMED; Aldrich). Upon washing with pure water, the hydrolyzed PCCA swelled dramatically ($\lambda_{\text{max}} > 1000$ nm).

The hydrolyzed PCCA was placed in a 25-mL aqueous solution of 5-amino-8-hydroxyquinoline (0.15 g, 0.64 mmol, Aldrich) and

- (12) Reese, C. E.; Guerrero, C. D.; Weissman, J. M.; Lee, K.; Asher, S. A. *J. Colloid Interface Sci.* **2000**, 232, 76–80.
- (13) Flaugh, P. L.; O'Donnell, S. E.; Asher, S. A. *Appl. Spectrosc.* **1984**, 38, 847–850.
- (14) Rundquist, P. A.; Photinos, P.; Jagannathan, S.; Asher, S. A. *J. Chem. Phys.* **1989**, 91, 4932–4941.
- (15) Asher, S. A.; Holtz, J.; Liu, L.; Wu, Z. *J. Am. Chem. Soc.* **1994**, 116, 4997–4998.
- (16) Holtz, J. H.; Asher, S. A. *Nature* **1997**, 389, 829–832.
- (17) Holtz, J. H.; Holtz, J. S. W.; Munro, C. H.; Asher, S. A. *Anal. Chem.* **1998**, 70, 780–791.
- (18) Asher, S. A.; Holtz, J. H.; Weissman, J. M.; Pan, G. *MRS Bull.* **1998**, (October), 44–50.

- (19) Markov, K.; Markova, N.; Mitev, S.; Damyanov, N. *God. Vissh. Khim.-Tekhnol. Inst., Sofia* **1977**, 22, 129–139.

1-ethyl-3-(3-dimethylaminopropyl)carbodiimide hydrochloride (EDC; 0.20 g, 1.04 mmol, Pierce) for 90 min. After washing in pure water, the PCCA diffraction maximum returned to nearly its value prior to hydrolysis.

Diffraction Measurements. The metal ion stock solutions were prepared by dissolving $\text{Cu}(\text{NO}_3)_2 \cdot 2.5\text{H}_2\text{O}$ (0.5815 g, 2.5 mmol, Fisher) in 50 mL of sodium acetate (Fisher) buffered saline. The pH was adjusted to 4.2 by addition of 20% aqueous NaOH (Fisher). Lower Cu^{2+} concentrations were prepared by successive dilution of the stock solution.

The PCCACS, as made, are extremely sticky; we touch the PCCACS to the polystyrene Petri dish surface to which it adheres. The other PCCACS surface is now situated for exposure to the sample solution. The pure water bathing the PCCACS for storage was replaced with 30 mL of acetate-buffered saline at pH 4.2, and the PCCACS was allowed to equilibrate. A diffraction red shift occurs as the ion concentrations equilibrate between the hydrogel and the buffer solution over a period of 5 min.

We then replaced the buffer solution with a buffer solution containing a defined analyte concentration. The response time of the PCCACS to each metal ion concentration (the time required for the diffraction peak to reach a stable value) depends on the metal cation concentration. The response time is, of course, longest (~ 6 h) for the lowest metal ion concentrations (where all ions in solution have to enter the PCCACS) but is considerably shorter for the higher concentrations (~ 5 min). We usually waited for ~ 30 min to ensure equilibrium, before measuring the diffraction maximum.

After treatment with the highest metal ion concentration solution, the PCCACS was washed five times for at least 20 min with 30-mL aliquots of acetate-buffered saline at pH 4.2. After washing was completed, the PCCACS was stored in buffered saline at pH 4.2.

RESULTS AND DISCUSSION

Response of PCCACS to Cu^{2+} . Replacement of the water in contact with the 8-hydroxyquinoline PCCACS ($1\text{ cm} \times 1\text{ cm} \times 125\text{ }\mu\text{m}$) with an aqueous saline acetate buffer at pH 4.2 (150 mM NaCl, 50 mM NaOAc, concentrated HCl to adjust pH) caused the diffraction to red shift ~ 40 nm from 717 to 757 nm. This red shift results from PCCACS hydrogel swelling, presumably due to an increased free energy of mixing of the hydrogel due to binding of Na^+ to the neutral phenolic groups of the 8-hydroxyquinoline sites;²⁰ Izzat et al.²⁰ previously observed alkali and alkaline earth cation binding to neutral 8-hydroxyquinoline derivatives. As shown in Figure 2, replacement of the pure saline buffer solution by a 30-mL solution containing 11 nM Cu^{2+} solution (0.68 ppb) results in a diffraction blue shift, from 757 to 705 nm. The diffraction maximum continues to blue shift as higher concentrations of Cu^{2+} are added. For example, subsequent addition of 30 mL of a 0.54 μM Cu^{2+} saline buffer solution caused the diffraction maximum to blue shift to 520 nm (green). Addition of 1 μM Cu^{2+} caused a further blue shift to 515 nm (green). In contrast, further increases in Cu^{2+} concentration resulted in diffraction red shifts. 2 μM Cu^{2+} results in diffraction at 533 nm (green); 54 μM Cu^{2+} results in diffraction at 547 nm (green-yellow); 0.5 mM Cu^{2+} results in

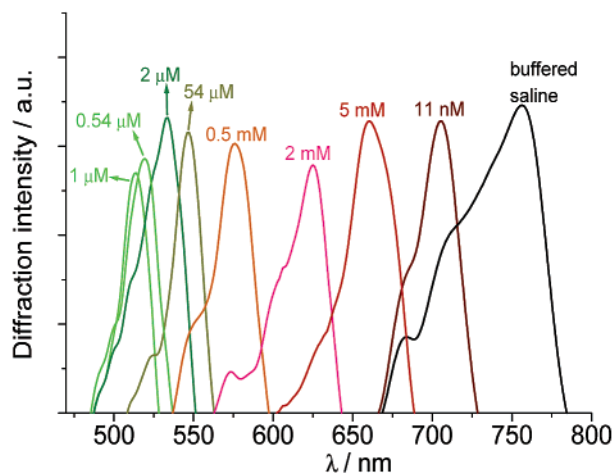


Figure 2. Diffraction dependence of the 8-hydroxyquinoline PC-CACS upon the Cu^{2+} concentrations of added 30-mL aqueous buffered saline solutions at pH 4.2.

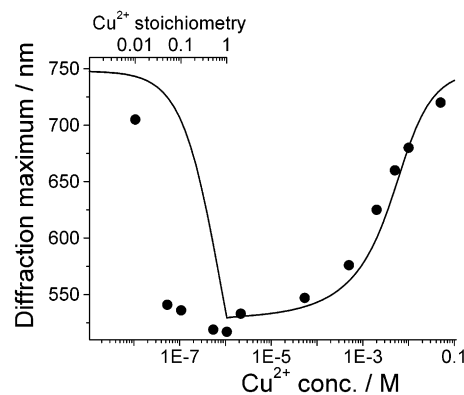


Figure 3. Dependence of the PCCACS diffraction wavelength maximum on the added amount of Cu^{2+} . The solid line is a theoretical fit using the model discussed below. The lower abscissa labels the Cu^{2+} concentrations of the added 30-mL solutions. The upper abscissa labels the added Cu^{2+} in terms of the relative stoichiometries of added Cu^{2+} relative to half of the total amount of the 8-hydroxyquinoline ligand sites.

diffraction at 576 nm (yellow-orange); 2 mM Cu^{2+} results in diffraction at 625 nm (red); and 5 mM Cu^{2+} results in diffraction at 660 nm (deep red). The diffraction maximizes at ~ 720 nm at even higher Cu^{2+} concentrations.

8-Hydroxyquinoline has extraordinarily large association constants^{21–23} for monoligated ($10^{10.70}\text{ M}^{-1}$) and bisliganded (10^{22} M^{-2}) Cu^{2+} complexes. Thus, we expect that at low concentrations Cu^{2+} binds as bisliganded complexes, which additionally cross-link the gel and causes the gel to shrink (Scheme 2). In contrast, at higher Cu^{2+} concentrations, the Cu^{2+} binds as monoligated complexes in which the cross-links are broken. This would explain the chevron-shaped Cu^{2+} titration curve (Figure 3). The formation of the bisliganded cross-links and the monodentate complexes is easily proven by comparing UV–visible absorption spectral Cu^{2+} titrations of 5-acetamido-8-hydroxyquinoline in solution and at

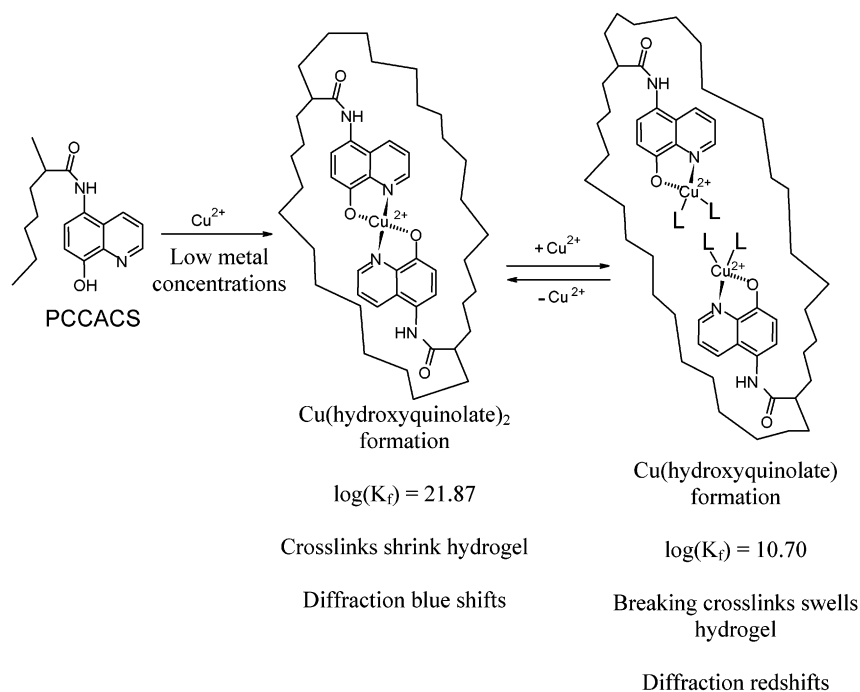
(20) Zhang, X. X.; Bordunov, A. V.; Bradshaw, J. S.; Dalley, N. K.; Kou, X.; Izzat, R. M. *J. Am. Chem. Soc.* **1995**, *117*, 11507–11511.

(21) *Lange's Handbook of Chemistry*, 11th ed.; Dean, J. A., Ed.; McGraw-Hill Publishers: New York, 1973; pp 5-57–5-58.

(22) Smith, R. M.; Martell, A. E. *Critical Stability Constants*. Vol. 2. *Amines*; Plenum Press: New York, 1975; pp 223–233.

(23) Richard, C. F.; Gustafson, R. L.; Martell, A. E. *J. Am. Chem. Soc.* **1959**, *81*, 1033–1040.

Scheme 2. Proposed Mechanism of Sensing of Cu^{2+} by 8-Hydroxyquinoline-Appended PCCACS



tached to a hydrogel in the absence of the CCA (Appendix 1). As discussed below (and shown by the solid line in Figure 3), we can quantitatively model the Cu^{2+} diffraction dependence by using the 8-hydroxyquinoline association constants and modeling the hydrogel volume response. As shown in Appendix 2, we determined the total number of ligand sites attached to our PCCACS and can thus plot in Figure 3 the dependence of the diffraction as a function of the Cu^{2+} /ligand stoichiometry ($S = \text{Cu}^{2+}_{\text{mol}}/2 \text{ ligand}_{\text{mol}}$), where $\text{Cu}^{2+}_{\text{mol}}$ is the number of added moles of Cu^{2+} and $\text{ligand}_{\text{mol}}$ is the number of moles of ligand in the PCCACS.

Surprisingly, significant diffraction blue shifts occur under conditions $S = 0.01$, where few cross-links are formed. This large response, which is inconsistent with our modeling, is due to sequestering of the available Cu^{2+} within the outermost layer of the PCCACS film due to the binding of Cu^{2+} to the first ligands encountered.

Since our observed diffraction is contributed mainly from the outermost PCCACS layer, our measurement selectively monitors the hydrogel volume, which first sequesters the Cu^{2+} . This is clearly evident from the fact that diffraction measurements taken from the PCCACS surface bound to the Petri dish show a much smaller blue shift.

Washing the Cu^{2+} containing PCCACS with buffer causes the diffraction to blue shift as the bisliganded Cu^{2+} sites are re-formed. Thus, the diffraction does not return to the original value before Cu^{2+} addition but blue shifts to 520 nm. As a consequence, the response of the sensor is only partially reversible. It is impossible to remove the bisliganded Cu^{2+} from the hydrogel because the association constant of the 2:1 ligand/ Cu^{2+} sites is so large. Thus, this sensing material can be used as a dosimeter for ultratrace concentrations of Cu^{2+} (where we detect substoichiometric amounts of Cu^{2+}) or as a reversible sensor for Cu^{2+} and other metal cation concentrations above 1 μM (~ 100 ppb).

This PCCACS can be utilized to determine ultratrace amounts of Cu^{2+} . For example, a PCCACS that contains 10 mM 8-hydroxy-

quinoline should be able to easily detect 10^{-21} M Cu^{2+} under equilibrium conditions (reaching equilibrium would take a very long time). A small $1 \mu\text{m} \times 1 \mu\text{m} \times 1 \mu\text{m}$ cube of this PCCACS could be used to easily detect $\sim 10^6$ Cu^{2+} ions, since we would be able to easily detect the diffraction shift due to cross-linking of 10% of the ligands.

The PCCACS can also be used to reversibly sense $>1 \mu\text{M}$ Cu^{2+} . For example, Figure 4 shows the diffraction response of a Cu^{2+} cross-linked PCCACS to increasing Cu^{2+} concentrations in buffered saline at pH 4.2. Two sensing runs are shown to illustrate the reproducibility of the diffraction shift with increasing Cu^{2+} concentrations. Upon washing with buffered saline at pH 4.2, the PCCACS returns to the blue-shifted minimum diffraction.

Hydrogel Cross-Linking, Volume Phase Transitions, and Diffraction Dependence on Cu^{2+} . The PCCACS diffracts light from the fcc 111 plane of the embedded CCA. These planes are parallel to the film surface and this diffraction closely follows Bragg's law:

$$\lambda_o = 2nd \sin \theta$$

where the diffracted wavelength (λ_o , measured in air) depends on the 111 plane spacing (d) and the refractive index of the system (n), where θ is the Bragg glancing angle.^{9–18} We usually monitor the back-diffraction of normally incident light. Thus, $\lambda_o = 2nd$. Changes in the diffraction wavelength are caused by alterations in the volume of the PCCACS. Since d is proportional to the third root of the volume, $\lambda_o = 2nkV^{1/3}$.

We can model the dependence of the diffraction on the Cu^{2+} concentration by modeling the number of hydrogel cross-links formed and by considering the impact of these cross-links on the hydrogel volume. We modeled the PCCACS response to Cu^{2+} by

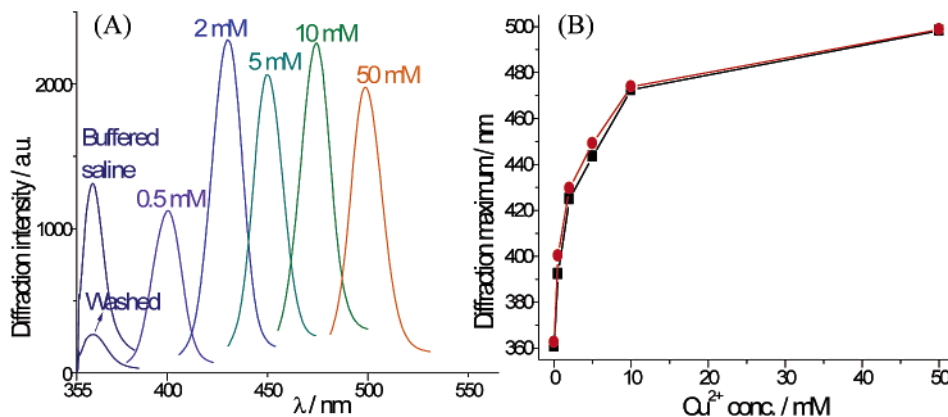


Figure 4. (A) Response of washed Cu²⁺ cross-linked 8-hydroxyquinoline PCCACS to increasing Cu²⁺ concentrations. (B) Two runs are presented to show the reproducible and reversible nature of the sensor response to Cu²⁺.

utilizing an improvement²⁴ to our previous models,^{25,26} which were based on Flory's ionic network model.²⁷ These models require that the total osmotic pressure at equilibrium must equal zero:

$$\Pi_T = \Pi_M + \Pi_E + \Pi_{\text{Ion}} = 0$$

Π_M and Π_E are the osmotic pressures associated with the free energy of mixing and with the network elasticity and Π_{Ion} is the osmotic pressure due to the difference in mobile ion concentration inside and outside the gel (Donnan potential):

$$\begin{aligned}\Pi_M &= -\frac{\partial \Delta G_M}{\partial V} = -\frac{RT}{V_s} \left[\ln \left(1 - \frac{V_0}{V} \right) + \frac{V_0}{V} + \chi \left(\frac{V_0}{V} \right)^2 \right] \\ \Pi_E &= -\frac{\partial \Delta G_E}{\partial V} = -\frac{RTn_{\text{cr}}}{V_m} \left[\left(\frac{V_m}{V} \right)^{1/3} - \frac{1}{2} \frac{V_m}{V} \right] \\ \Pi_{\text{Ion}} &= RT(c_+ + c_- - c_+^* - c_-^*)\end{aligned}\quad (1)$$

R is the universal gas constant, T is the temperature, χ is the Flory–Huggins interaction parameter for the polymer network and the solution, V_s is the molar volume of the solvent, n_{cr} is the effective number of cross-linked chains in the network, V is the existing volume of the gel, V_m is the volume of the relaxed network, V_0 is the volume of the dry polymer network, c_+ and c_- are the concentrations of cations and anions inside the gel, and c_+^* and c_-^* are the concentrations outside the gel. For high ionic strength solutions, the Donnan potential is negligible and at equilibrium:

$$\Pi_M + \Pi_E = 0$$

We ignore changes in χ upon Cu²⁺ binding, since the small free energy of mixing change is likely to be negligible compared to cross-linking changes. Thus, our main assumption is that the

change in hydrogel volume results solely from formation or breakage of Cu²⁺ cross-links in the hydrogel network.

To model the volume phase transition we need to separately treat the two types of hydrogel cross-links. The total number of cross-linked chains is $n_{\text{cr}} = n_{\text{cr}}^0 + 2 \cdot n_{\text{L}_2\text{M}}$, where n_{cr}^0 is the effective number of permanently cross-linked chains formed during the original polymerization of the network and $n_{\text{L}_2\text{M}}$ is the number of additional cross-linked chains due to Cu²⁺ complexation to 8-hydroxyquinoline ligand sites.

The original cross-links formed during PCCA polymerization required the chains to adopt their most probable chain configurations at the original PCCA volume. However, the Cu²⁺ cross-links form at varying hydrogel volumes. If these additional cross-links show reversible Cu²⁺ binding, or exchange, we assume that they relax to their most probable configurations at any hydrogel volume.

If we explicitly recognize this difference in the nature of the cross-links, we conclude that the osmotic pressure arising from network elasticity is

$$\Pi_E = -\frac{\partial \Delta G_E}{\partial V} = -\frac{RTn_{\text{cr}}^0}{V_m} \left[\left(\frac{V_m}{V} \right)^{1/3} - \frac{1}{2} \frac{V_m}{V} \right] - RTc_{\text{L}_2\text{M}}$$

where $c_{\text{L}_2\text{M}}$ is the concentration of the additional cross-links ($c_{\text{L}_2\text{M}} = n_{\text{L}_2\text{M}}/V$).

We can calculate the volume of the hydrogel (and the diffracted wavelength) at each Cu²⁺ concentration by calculating the number of Cu²⁺/8-hydroxyquinoline cross-links formed, as indicated in Appendix 3.

Our best-fit modeling required a Flory–Huggins interaction parameter of $\chi = 0.49$ and a value of $n_{\text{cr}}^0/V_m = 5.9 \times 10^{-4}$ M. The slightly decreased χ value from the $\chi = 0.495$ used previously for a boronic acid glucose PCCA^{24,26} indicates a more favorable free energy of mixing for this PCCACS material. The best-fit value of n_{cr}^0/V_m is 20% below the value we expected; our PCCACS utilized only half the cross-linker concentration used previously,²⁵ and we assume that this would result in the formation of half the previous cross-link density.

We initially started fitting our model by using the literature association constants^{21–23} of $K_1 = 10^{10.70}$ and $K_3 = 10^{20.92}$. However, our best fit found that $K_4 = (K_1)^2/K_3 = 10^{0.44}$ instead of the

- (24) Alexeev, V. L.; Sharma, A. C.; Goponenko, A. V.; Das, S.; Lednev, I. K.; Wilcox, C. S.; Finegold, D.; Asher, S. A. *J. Am. Chem. Soc.* Submitted.
 (25) Lee, K.; Asher, S. A. *J. Am. Chem. Soc.* **2000**, *122*, 9534–9537.
 (26) Asher, S. A.; Alexeev, V. L.; Goponenko, A. V.; Sharma, A. C.; Lednev, I. K.; Wilcox, C.; Finegold, D. *J. Am. Chem. Soc.* Submitted.
 (27) Flory, P. J. *Principles of Polymer Chemistry*; Cornell University Press: Ithaca, NY, 1953.

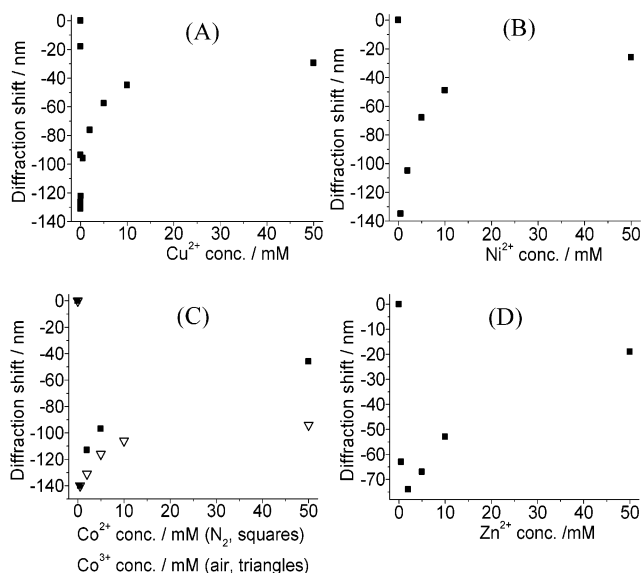


Figure 5. Dependence of 8-hydroxyquinoline PCCACS diffraction on increasing metal ion concentrations: (A) Cu^{2+} ; (B) Ni^{2+} ; (C) Co^{2+} (N_2 , squares) and Co^{3+} (air, triangles); (D) Zn^{2+} .

literature $K_4 = 10^{-0.47}$. Presumably, changes in the bound 8-hydroxyquinoline ligand association constants are induced by the PCCA environment.

Our model excellently fits the measured response of our sensor to Cu^{2+} for exposure to samples with concentrations greater than $1 \mu\text{M}$ (Figure 3). As discussed above, we are unable to measure equilibrium responses to Cu^{2+} concentrations below $1 \mu\text{M}$ due to the inconvenience of working with the large sample volumes required.

8-Hydroxyquinoline PCCACS is a Nonspecific Metal Cation Sensor. 8-Hydroxyquinoline derivatives are promiscuous cation ligands that display high association constants to a wide range of metal ions in aqueous solution.^{21–23} Figure 5 shows that the 8-hydroxyquinoline PCCACS responds to Ni^{2+} in a manner essentially identical to that of Cu^{2+} as discussed above. This is expected in view of the high Ni^{2+} association constants, $K_1 = 10^{9.57}$ and $K_3 = 10^{18.27}$. The PCCACS, under an inert atmosphere of N_2 , responds to Co^{2+} in a manner essentially identical to that of Cu^{2+} and Ni^{2+} . This is expected, in light of the high Co^{2+} association constants, $K_1 = 10^{8.11}$ and $K_3 = 10^{15.05}$.

However, a different response is observed if measured in air. Although, the low cation concentration blue shift of the PCCACS diffraction is similar to that for Cu^{2+} , Ni^{2+} , and Co^{2+} (under N_2), a much lower diffraction red shift occurs for the higher Co^{2+} concentrations (in air) than for the higher concentrations of Cu^{2+} , Ni^{2+} , and Co^{2+} (under N_2). Presumably, this results from oxidation²⁸ of 8-hydroxyquinoline-bound Co^{2+} to 8-hydroxyquinoline-bound Co^{3+} . The red shift decrease probably results from a decreased affinity of Co^{2+} for 8-hydroxyquinoline-bound Co^{3+} .

Zn^{2+} causes a 2-fold smaller blue shift at low concentrations. However, at higher concentrations, it gives rise to red shifts almost back to the original diffraction wavelength, much like Cu^{2+} , Co^{2+} , and Ni^{2+} . It is difficult to understand the differences between Zn^{2+} and these other metals, if the bound 8-hydroxyquinoline has association constants^{21–23} similar to those reported for the free

ligand of $K_1 = 10^{8.65}$ and $K_3 = 10^{16.15}$. Even though the association constants are the lowest among the metals studied, they are still sufficiently high that we expect PCCACS responses similar to Cu^{2+} , Co^{2+} , and Ni^{2+} .

It is likely that the effective Zn^{2+} association constants for hydrogel-bound 8-hydroxyquinoline are decreased compared to that of free 8-hydroxyquinoline; the hydrogel constraints would cause a much larger entropy penalty, ligand geometry constraint, or both, which would decrease its affinity compared to the free ligand.

Indeed, a lower Zn^{2+} association constant is indicated from the observation that washing removes Zn^{2+} from the hydrogel; the diffraction red shifts. In fact, Ca^{2+} , which has a value of $K_1 = 10^{3.5}$, readily washes out of the PCCACS.

CONCLUSIONS

We have fabricated a novel sensing material for the detection of ultratrace concentrations of metal cations such as Cu^{2+} , Ni^{2+} , Co^{2+} , Co^{3+} , Ca^{2+} , and Zn^{2+} , as well as other cations with similar 8-hydroxyquinoline association constants,^{21–23} which include Th^{4+} , Sm^{3+} , Fe^{3+} , Gd^{3+} , and Er^{3+} . We will examine the detection of these species in a future publication.

At low metal concentrations ($< \mu\text{M}$), the cations form bisliganded complexes with two 8-hydroxyquinolines, which cross-link the gel, and cause the hydrogel to shrink and blue shift the diffraction. At higher metal concentrations, monoliganded complexes form that break the bisliganded cross-links and the diffractions red shift. We have extended hydrogel volume phase transition theory in order to quantitatively model the metal cation concentration diffraction dependence. These materials can be used as dosimeters to sense extremely low metal cation concentrations ($\sim 10^{-21} \text{ M}$) or as sensor materials for concentrations greater than $1 \mu\text{M}$. Metal cation concentrations can be determined visually from the color of the diffracted light or detected by reflectance measurements using a spectrophotometer. This sensing material should be easily usable in the field to evaluate metal concentrations in drinking water. The readout could utilize visual estimation of the diffraction with the aid of a color chart.

APPENDIX 1

We can demonstrate the formation of the bis- and monoliganded Cu^{2+} /8-hydroxyquinolate complexes in our hydrogel by comparing the absorption spectrum of a hydrogel to that of solution Cu^{2+} complexes of 5-acetamido-8-hydroxyquinoline. Figure 6A shows that the formation of the bisliganded 1:2 Cu (5-acetamido-8-hydroxyquinolate)₂ red shifts the $\sim 250\text{-nm}$ absorption to $\sim 270 \text{ nm}$ and creates a new absorption band at 380 nm . Further addition of Cu^{2+} forms the 1:1 Cu (5-acetamido-8-hydroxyquinolate) complex, which gives rise to smaller spectral changes such as a small blue shift in the 380-nm absorption band and an increased absorbance at $\sim 300 \text{ nm}$. The similar hydrogel absorption spectral changes (Figure 6B) prove the formation of the bisliganded and monoliganded complexes at low and high Cu^{2+} levels. Cu^{2+} is not retained by a similar PCCA, which does not contain 8-hydroxyquinoline pendent groups, as shown by AA spectroscopy. This also indicates the formation of very high affinity Cu^{2+} binding sites within the hydrogel that involve the pendent 8-hydroxyquinoline groups.

(28) Guesnet, P.; Bauer, D. J. *Chem. Res., Synop.* **1981**, 5, 127.

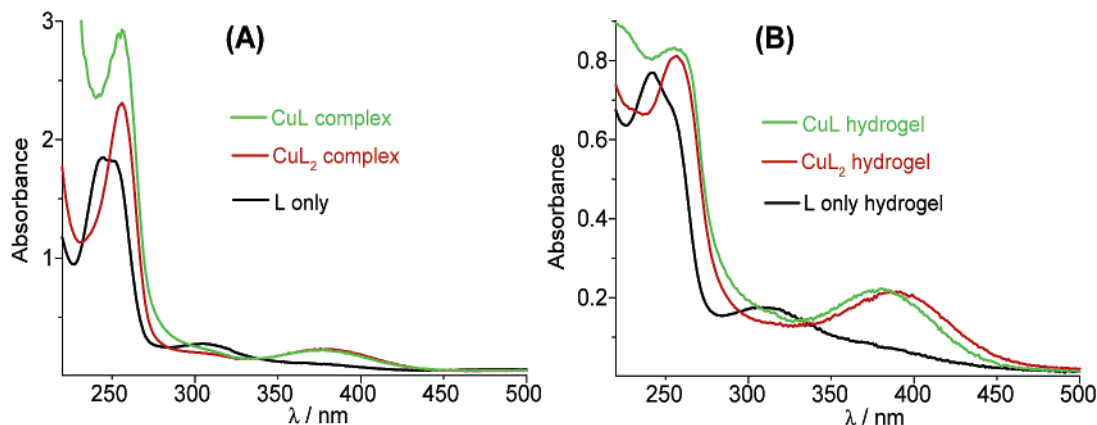


Figure 6. UV–visible Cu^{2+} titration of (A) 5-acetamido-8-hydroxyquinoline in acetate-buffered saline and (B) 8-hydroxyquinoline-functionalized CCA-free hydrogel in buffered saline at pH 4.2.

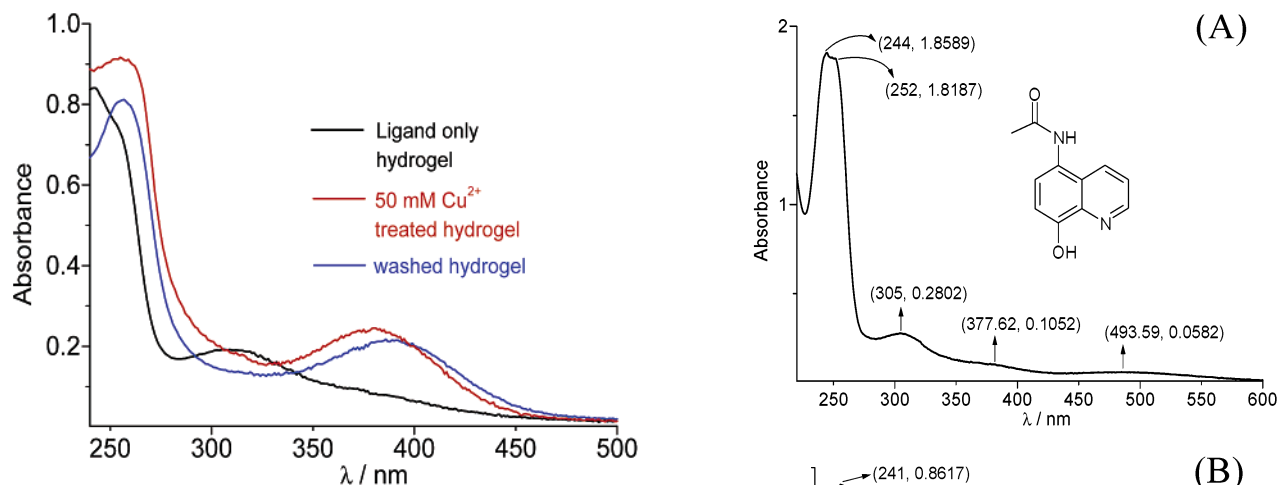


Figure 7. UV–visible absorption spectra of CCA free 8-hydroxyquinoline polyacrylamide hydrogel, which shows retention of bisliganded Cu^{2+} sites after extensive washing with pH 4.2 buffered saline.

Figure 7 demonstrates that we are unable to wash out the bisliganded Cu^{2+} . After washing, we still observe the absorption spectral features of the bisliganded complex as show in Figure 6 above.

APPENDIX 2

We determined the concentration of 8-hydroxyquinoline attached to the PCCACS by preparing a colloid-free, nondiffracting, 8-hydroxyquinoline hydrogel and using UV–visible absorption spectroscopy. Figure 8 compares the absorption spectrum of 5-acetamido-8-hydroxyquinoline to that of an 8-hydroxyquinoline-functionalized colloid-free hydrogel. For the peaks at 244, 252, 305, and 377 nm in the spectrum of 5-acetamido-8-hydroxyquinoline in acetate-buffered saline at pH 4.2, we calculate molar extinction coefficients of 1.86×10^4 , 1.82×10^4 , 2.80×10^3 , and $1.05 \times 10^3 \text{ M}^{-1} \text{ cm}^{-1}$, respectively. Assuming identical molar extinction coefficients for the analogous peaks of 8-hydroxyquinoline attached to the colloid-free gel in acetate-buffered saline at pH 4.2, we calculate a ligand concentration of 5.2 mM in the colloid-free hydrogel. Since identical conditions were employed to prepare the metal ion sensor PCCACS, we expect an identical 8-hydroxyquinoline concentration.

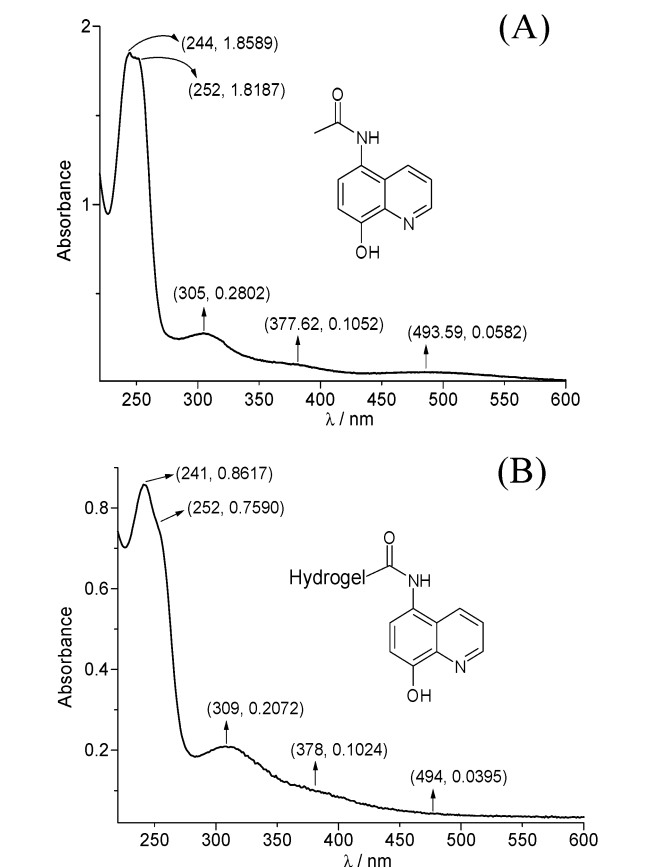
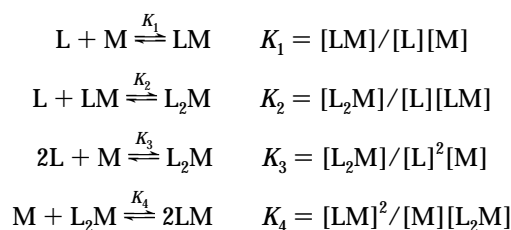


Figure 8. UV–visible spectra of (A) 5-acetamido-8-hydroxyquinoline and (B) colloid-free 8-hydroxyquinoline-containing hydrogel, both in buffered saline at pH 4.2.

APPENDIX 3

The number of cross-links formed at any Cu^{2+} concentration can be determined from the four equilibria involving the possible Cu^{2+} /8-hydroxyquinoline complexes.



where L = 8-hydroxyquinoline, M = Cu²⁺, LM = Cu(8-hydroxyquinolate)⁺ 1:1 complex, and L₂M = Cu(8-hydroxyquinolate)₂ bisliganded complex. These equilibrium constants are known from previous studies.^{21–23}

The total concentration (c_T) of 8-hydroxyquinoline ligands in the hydrogel is

$$c_T = [L] + K_1[L][M] + 2K_3[L]^2[M] = n_T/V$$

while the concentration of Cu(8-hydroxyquinolate)₂ bisliganded cross-links (c_{L₂M}) is

$$c_{L_2M} = [L_2M] = K_3[L]^2[M]$$

n_T is the total amount of 8-hydroxyquinolate in the PCCACS and [M] is the Cu²⁺ concentration in the solution. The free metal ion concentration in solution is depleted due to complexation:

$$V_{\text{res}}c_M = [M](V_{\text{res}} + V) + (K_1[L] + K_3[L]^2)[M]V$$

c_M is the initial concentration of metal ion in the solution and V_{res} is the volume of the solution added (the reservoir volume). If c_MV_{res} ≫ c_TV, we can assume that [M] = c_M.

ACKNOWLEDGMENT

We gratefully acknowledge financial support from NIH Grant DK55348, ONR Grant N00014-94-1-0592, and DOE Grant DEFG0798ER62708. We are grateful to Mr. Chad Reese, who generously supplied us with abundant amounts of polystyrene latex CCAs. We especially thank Professor Rex Shepherd from the University of Pittsburgh for helpful comments about ligand binding, and Professor Mark Meyerhoff from the University of Michigan for insights about cobalt oxidation.

Received for review November 19, 2002. Accepted January 27, 2003.

AC026328N